Role of CB 1 receptors in the gastrointestinal tract after microbiota depletion and natural recolonization

Evandro J. Beraldi
University of Calgary
Yasaman Bahojb Habibyan
University of Calgary
Catherine M. Keenan
University of Calgary
Laurie E. Wallace
University of Calgary
Keith A. Sharkey
ksharkey@ucalgary.ca
University of Calgary

Article

Keywords: endocannabinoids, intestinal transit, myenteric plexus, submucosal plexus

Posted Date: March 16th, 2026

DOI: https://doi.org/10.21203/rs.3.rs-8854797/v1

Additional Declarations: No competing interests reported.

Role of CB_1 receptors in the gastrointestinal tract after microbiota depletion and natural recolonization

Evandro J. Beraldi, Yasaman Bahojb Habibyan, Catherine M. Keenan, Laurie E. Wallace, Keith A. Sharkey (ORCiD ID: 0000-0001-9560-1711)*

Hotchkiss Brain Institute, Snyder Institute for Chronic Diseases and Department of Physiology & Pharmacology, Cumming School of Medicine; University of Calgary, Alberta, Canada

*Corresponding author

Word count: 3789 (Main text, excluding Methods, Figure Legends, Tables and References)

Short title: Role of CB_1 receptors in the GI tract after microbiota recolonization

*Author for correspondence:

Dr. Keith Sharkey
Department of Physiology and Pharmacology
Cumming School of Medicine
University of Calgary
3330 Hospital Drive NW
Calgary, AB T2N 4N1 Canada

Phone: (403) 220-4601

Email: ksharkey@ucalgary.ca

Abstract

The endocannabinoid system is involved in the control of gastrointestinal motility and function, with increasing evidence of its interactions with gut microbiota. We investigated if cannabinoid $(CB)_1$ receptors participate in the enteric nervous system (ENS) response to microbiota depletion and natural microbial recolonization. We characterized enteric neurons and glia in the ileum and colon of CB_1 receptor knockout mice (CB_1-KO), showing their ENS is identical to wild type (WT) mice. Next, WT and CB_1-KO mice were treated for 2 weeks with antibiotics followed by 2 or 4 weeks of natural microbial recolonization, compared to mice on water or continuous antibiotic treatment. CB_1-KO mice lost significantly more body weight than WT mice during antibiotic treatment, and both genotypes had slower whole gut transit with antibiotic treatment. Compared to WT mice, CB_1-KO mice had faster whole gut transit, but slower colonic motility after recolonization. Gut microbiota diversity was similarly affected by antibiotic treatment in both genotypes. CB_1-KO mice showed the same ENS neuronal and glial density as WT mice in all populations, with neuronal loss after antibiotic treatment and recovery after natural microbial recolonization. Altogether, this study reveals new insights in the interactions between the endocannabinoid system and gut microbiota in gastrointestinal function.

Keywords: endocannabinoids, intestinal transit, myenteric plexus, submucosal plexus, enteric glia, enteric neurons.

Introduction

The gastrointestinal (GI) tract contains the largest microbial ecosystem in the body [1,2]. The gut microbiota is being increasingly recognized to play important roles in the regulation of GI function [3-7], as well as nutrition, immune homeostasis, and metabolism [8-12]. Gut function is controlled and coordinated by the enteric nervous system (ENS) [5]. Located in the wall of the gut, the ENS provides precise temporal and spatial control of digestion and host defense, in part through two-way interactions with the gut microbiota [5,13,14]. Overall, this bidirectional signaling contributes to the enteric neural control of gut physiology and the composition of the gut microbiota.

The endocannabinoid system plays important roles in the control of gut physiology via the lipid mediators anandamide and 2-arachidonoylglycerol (2-AG), and cannabinoid $(CB)_1$ and CB_2 receptors located on the intestinal epithelium, immune cells and enteric nerves [15-18]. There are important interactions between endocannabinoids, CB receptors and the gut microbiota, which are also a source of endocannabinoids and their metabolic enzymes [19-25]. In particular, CB_1 receptors are found throughout the ENS, where they modulate GI motility by providing inhibitory control of neurotransmission, slowing GI transit [26,27]. Whether CB_1 receptors influence the development and the structure of the ENS [28,29], as they do in the central nervous system (CNS), remains to be determined.

Mice treated with broad-spectrum antibiotics to deplete gut bacteria have altered GI structure and function, including slower transit time and loss of enteric neurons in both the small and large intestine [14,30-33]. These effects can be reversed by natural bacterial recolonization, confirming the microbiota as a critical determinant of ENS allostasis and gut function [14]. Since the endocannabinoid system is involved in the control of GI motility, secretory and barrier function and interactions with the gut microbiota [15-17], we hypothesized that CB_1 receptors participate in the response to natural recolonization, and that mice lacking CB_1 receptors would demonstrate altered functional responses to natural bacterial recolonization compared to wild type animals.

We tested this hypothesis by investigating the response to bacterial depletion and recovery of the ENS, as well as secretory, motor and barrier function after natural microbial recolonization using CB_1 receptor knockout mice. This allowed us to characterize the structure of the ENS in the absence of endocannabinoid signalling via CB_1 receptors in animals without any overt gut pathology, e.g. inflammation. Our results reveal that CB_1 receptors do not appear to influence the overall structure of the ENS but are involved in the control of GI motility in response to bacterial depletion and natural microbial recolonization.

Results

The GI tract and ENS in CB_1 receptor knockout mice

Before determining the response of CB_1 receptor knockout mice to microbial depletion and natural microbial recolonization, we first examined the general structure of the GI tract and ENS in CB_1 knockout mice, and compared it to wild type controls, as this has not been described previously. There were no differences in the length of the small or large intestine between male or female mice in either of these two groups of mice (Supplementary Figure 1).

Supplementary Figure 1

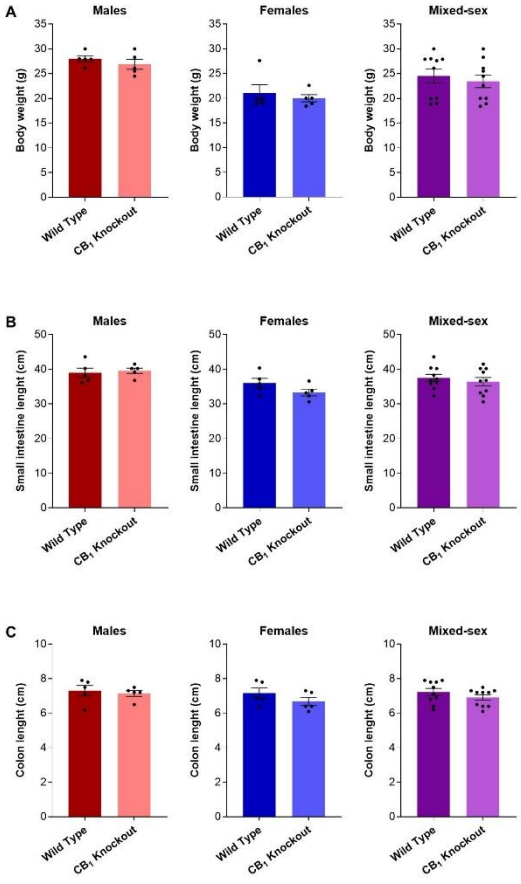

Supplementary Figure 1. Body weight, small intestinal and colonic length in CB_1 receptor knockout mice

Males, females and mixed-sex wild type or CB_1 receptor knockout mice were compared. **A.** Body weight. **B.** Small intestine length. **C.** Colon length. Mean ± SEM, groups compared with

Student's t-test, n = 5-10/group. There were no significant differences between any of the groups.

Similarly, there were no significant differences in the total numbers of enteric neurons (HuC/D$^+$ cells), enteric glia (S100B$^+$ cells), excitatory enteric neurons expressing choline acetyltransferase (ChAT$^+$) or inhibitory neurons expressing neuronal nitric oxide synthase (nNOS$^+$) in the myenteric plexus of the ileum or colon (Figure 1A-D, Supplementary Figure 2A), or enteric neurons (HuC/D$^+$), and enteric glia (S100B$^+$) in the submucosal plexus of the ileum or colon between males and females in these two groups of mice (Figure 2A-B, Supplementary Figure 2B).

Figure 1

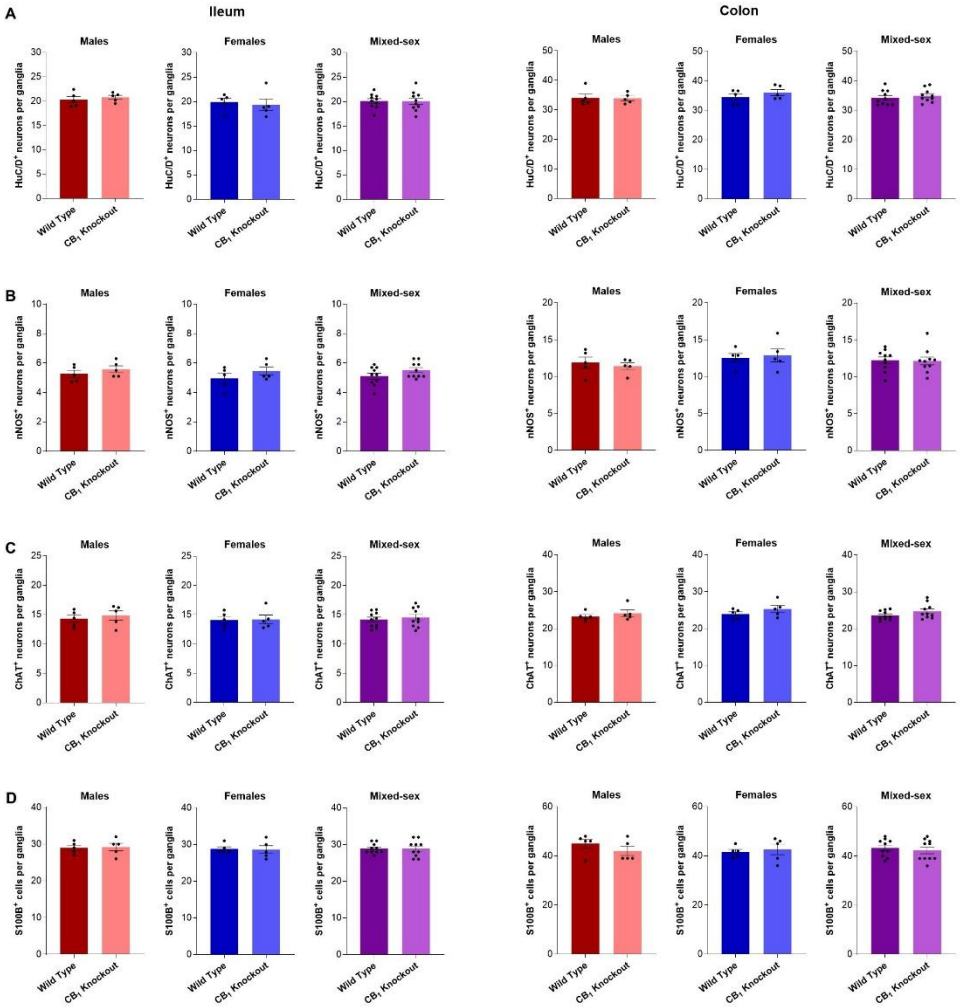

Figure 1. Neuronal and glial density in the myenteric plexus of CB_1 receptor knockout mice. Cell density in the myenteric plexus of the ileum and colon of CB_1 knockout mice compared to wild type control mice. Data were analysed comparing males, females and mixed-sex mice of both genotypes. **A.** HuC/D$^+$ neurons per ganglia. **B.** Neuronal nitric oxide synthase (nNOS$^+$) neurons per ganglia. **C.** Choline acetyltransferase (ChAT$^+$) neurons per ganglia. **D.** S100B$^+$ enteric glial cells per ganglia. Mean ± SEM, groups compared with Student's t-test, n = 5-10/group. There were no significant differences between any of the groups.

Figure 2

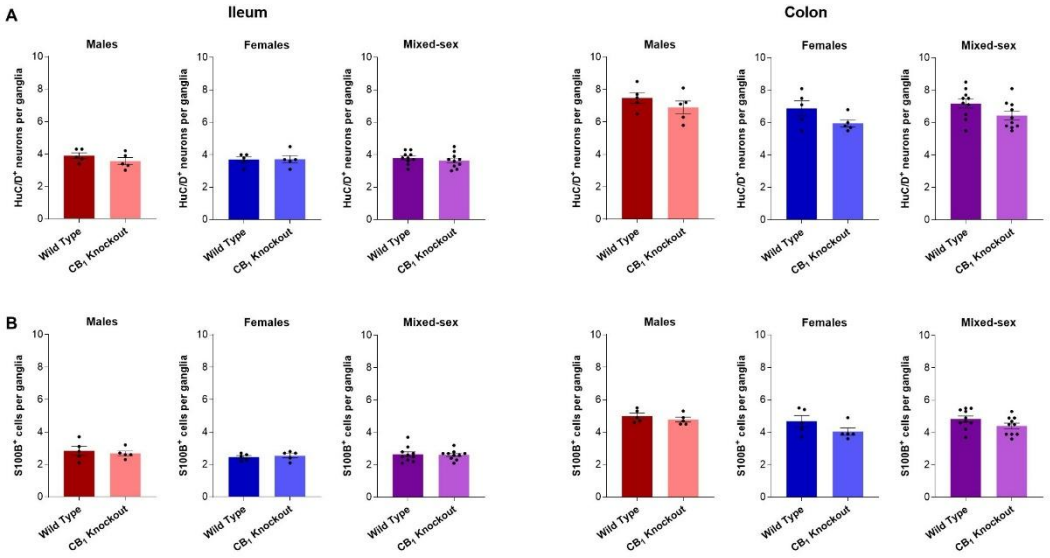

Figure 2. Neuronal and glial density in the submucosal plexus of CB_1 receptor knockout mice Cell density in the submucosal plexus of the ileum and colon of CB_1 knockout mice compared to wild type control mice. Data were analysed comparing males, females and mixed-sex mice of both genotypes. **A.** HuC/D$^+$ neurons per ganglia. **B.** S100B$^+$ enteric glial cells per ganglia. Mean ± SEM, groups compared with Student's t-test, n = 5-10/group. There were no significant differences between any of the groups.

Supplementary Figure 2

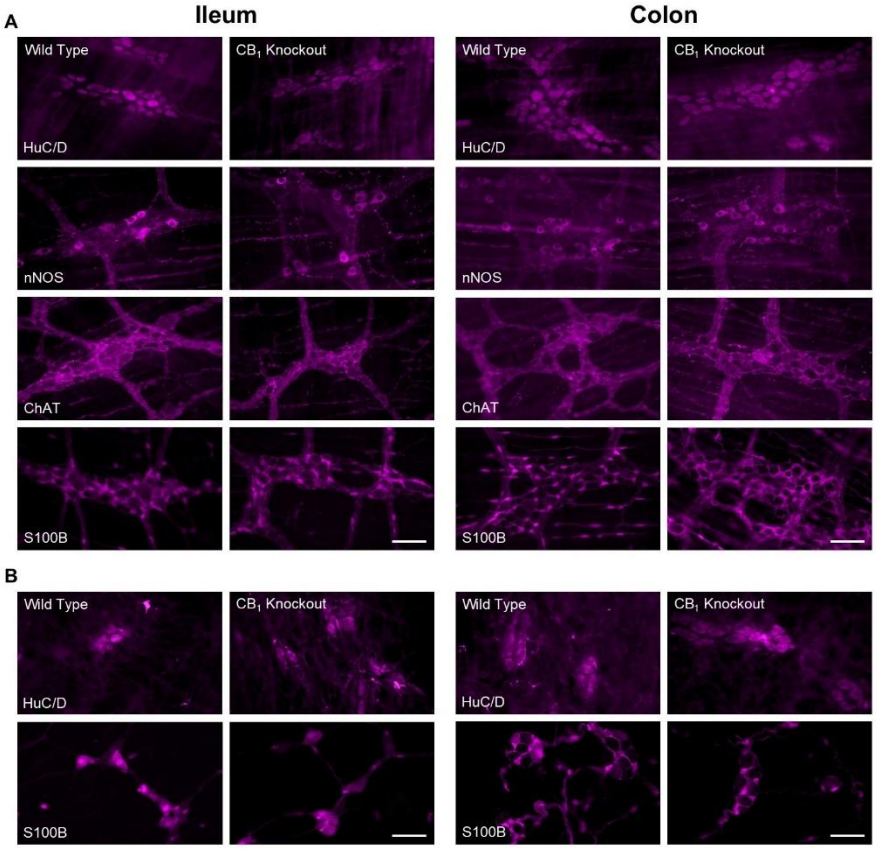

Supplementary Figure 2. ENS structure in wild type and CB_1 receptor knockout mice

Representative images of the ENS in the ileum and colon of mixed-sex wild type and CB_1 knockout mice. **A.** Single-labeling immunofluorescence in the myenteric plexus for HuC/D$^+$ neurons, neuronal nitric oxide synthase (nNOS$^+$) neurons, choline acetyltransferase (ChAT$^+$) neurons and S100B$^+$ glial cells. Scale bar: 30 µm. **B.** Single-labeling immunofluorescence in the submucosal plexus for HuC/D$^+$ neurons and S100B$^+$ enteric glial cells. Scale bar: 15 µm.

The effects of antibiotic administration on bacterial load, composition, and body weight

We then administered an antibiotic cocktail for 14 days to mixed sex groups of wild type and CB_1 receptor knockout mice and allowed natural recolonization following cessation of the antibiotic, comparing them to animals that were maintained on antibiotic for the duration of the experiment, or to animals not receiving any treatment (Figure 3A). Wild type mice lost very little weight when administered the antibiotic cocktail for 14 days and their rate of weight gain over time was very similar to that of untreated controls (Figure 3B), as we have previously published [14]. In contrast, CB_1 receptor knockout mice lost 10-15% of initial body weight and displayed a sustained reduction in body weight when maintained on antibiotics (Figure 3B). In a second study, we administered antibiotics for 14 days and then allowed a month for recolonization (Figure 3A). As expected, body weight progression was very similar to the experiments with 2 weeks of natural recolonization. Antibiotic-treated wild type mice lost very little weight and showed a stable progression over time, while CB_1 receptor knockout mice showed a significant reduction in body weight when treated with antibiotics (Figure 3C). In both studies, all mice lost a small amount of weight in the last week due to a degree of stress from the GI motility experiments.

Figure 3

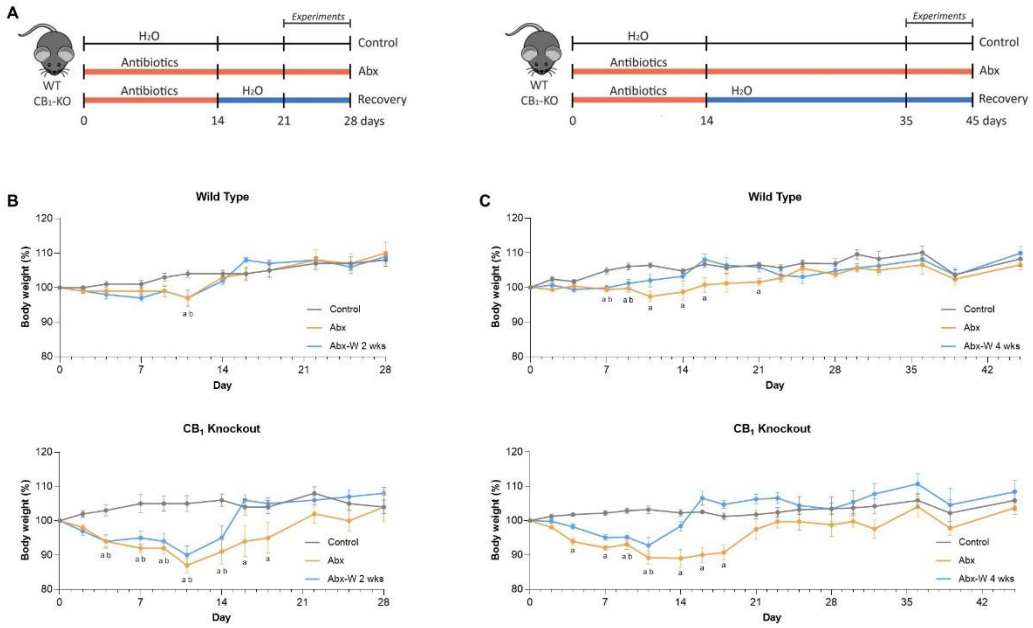

Figure 3. Experimental design and body weight progression in mice treated with antibiotics followed by natural microbial recolonization

A. Depletion of gut microbiota with antibiotics was performed on mixed-sex wild type (WT) and CB_1 receptor knockout mice (CB_1-KO). The antibiotic cocktail in drinking water was administered for 14 days, followed by regular drinking water for another 14 or 31 days (Recovery). The antibiotic (Abx)-treated group was maintained on antibiotic cocktail continuously throughout the experiment (28 or 45 days in total). GI motility experiments were performed in the last week of treatment in each study. **B.** Body weight progression of mixed-sex wild type and CB_1 receptor knockout mice maintained on water, continuous antibiotics (Abx) or antibiotics followed by 14 days of natural microbial recolonization (Abx-W 2 wks). Groups compared with two-way ANOVA followed by Sidak's multiple comparison test, n=7-9/group. $^{a}p < 0.05$ for Abx vs Control, $^{b}p < 0.05$ for Abx-W 2 wks vs Control. **C.** Body weight progression of mixed-sex wild type and CB_1 receptor knockout mice maintained on water, continuous antibiotics or antibiotics followed by 31 days of natural microbial recolonization (Abx-W 4 wks). Groups compared with two-way ANOVA followed by Sidak's multiple comparison test, n = 5-6/group. $^{a}p < 0.05$ Abx vs Control, $^{b}p < 0.05$ Abx-W 4 wks vs Control.

Antibiotic treatment significantly reduced fecal bacterial load after 2 weeks of treatment (Figure 4A). Following cessation of antibiotics for 2 weeks, there was a complete restoration of the fecal bacterial load in both wild type and CB_1 receptor knockout mice (Figure 4A). We determined that the cecal weight significantly increased in antibiotic-treated mice, as an indicator of successful bacterial elimination (Figure 4B). The magnitude of the increase was similar in both wild type and CB_1 receptor knockout mice, and both groups of mice saw a significant, but partial, recovery after antibiotic withdrawal. Interestingly, cecal weight in CB_1 receptor knockout mice was lower than wild type mice after antibiotic treatment and 2 weeks after cessation of treatment (Figure 4B). Four weeks after cessation of antibiotic treatment, the cecal weights of wild type and CB_1 receptor knockout mice were virtually indistinguishable.

Assessment of alpha (Simpson's and Shannon's indices) and beta (Bray-Curtis) diversity of the fecal microbiota revealed that there were no significant differences between wild type and CB_1 receptor knockout mice, in all experimental groups of animals (Figures 4C, 4D, 4E). Antibiotic treatment significantly reduced alpha diversity in both wild type and CB_1 receptor knockout mice; withdrawal of antibiotics led to the recovery of dominant taxa shown by Simpson's diversity analysis (Figure 4C). However, species richness and rare bacterial taxa were not completely recovered even a month after cessation of antibiotics, which was highlighted by Shannon's diversity analysis (Figure 4D). These differences were also reflected in the beta diversity plots (Figure 4E), where the wild type and CB_1 receptor knockout mice clustered very closely within the three experimental groups. All three experimental groups were significantly different, however, a shift towards control groups was apparent following withdrawal of antibiotics and only partially recovered 2 weeks after cessation of antibiotics (Figure 4E; note that very similar data was seen 4 weeks after cessation of antibiotic treatment, but due to a technical problem sample sizes were too low for statistical comparison).

Figure 4

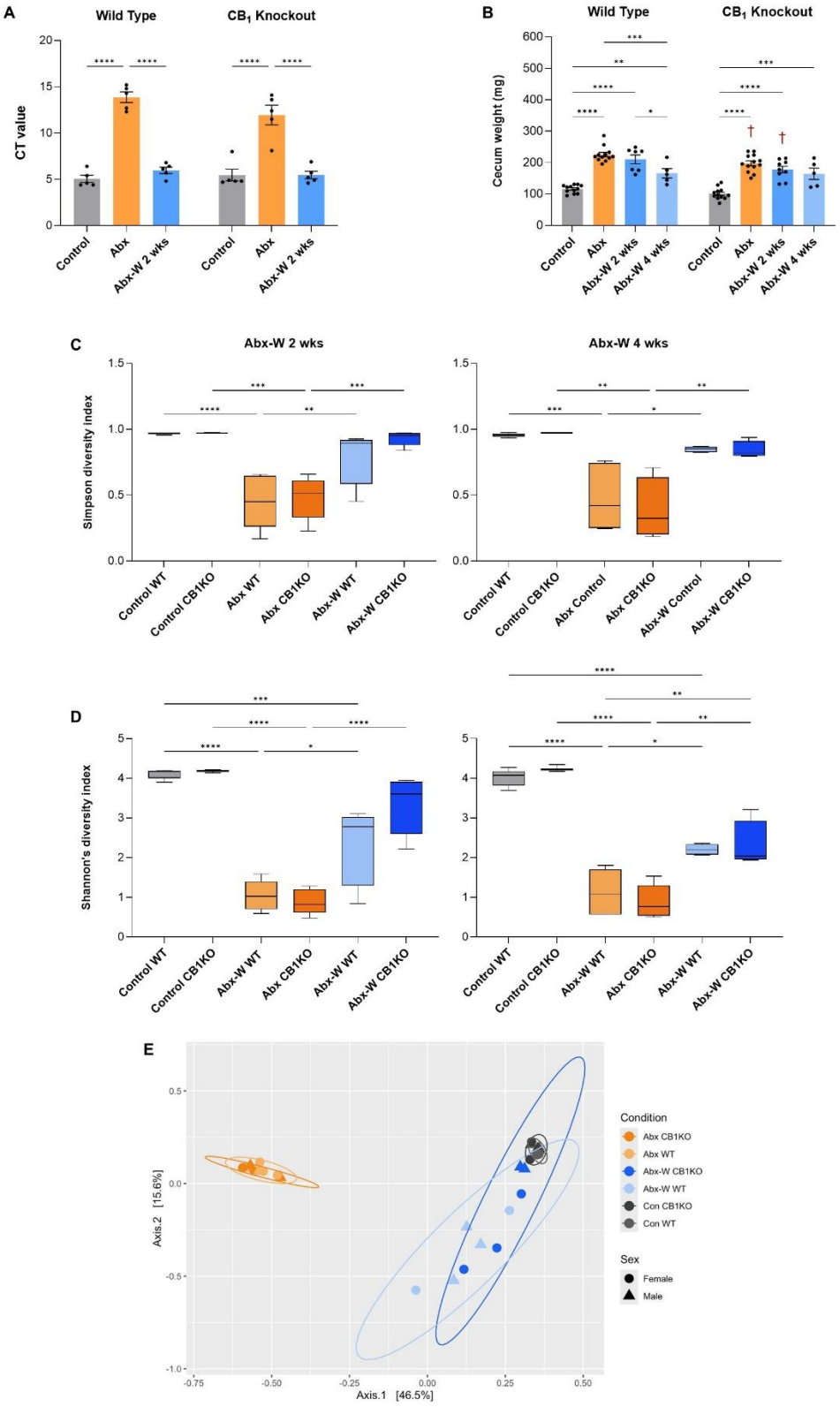
A
Wild Type
CB1 Knockout
CT value
Control
Abx
Abx-W 2 wks
B
Cecum weight (mg)
Abx-W 4 wks
C
Abx-W 2 wks
Abx-W 4 wks
Simpson diversity index
Control WT
Control CB1KO
Abx WT
Abx CB1KO
Abx-W WT
Abx-W CB1KO
Abx Control
Abx-W Control
D
Shannon's diversity index
E
Axis.1 [46.5%]
Axis.2 [15.6%]
Condition
Abx CB1KO
Abx WT
Abx-W CB1KO
Abx-W WT
Con CB1KO
Con WT
Sex
Female
Male

Figure 4. Fecal bacteria load, cecal weight and microbial diversity in mice treated with antibiotics followed by natural microbial recolonization

A. Fecal bacteria load of mixed-sex wild type and CB_1 receptor knockout mice after Abx treatment and after the natural recolonization 14 days after Abx withdrawal (Abx-W 2 wks). Data presented as mean ± SEM of qPCR Ct values. Groups compared with two-way ANOVA followed by Sidak's multiple comparison test, n = 5/group. ****p < 0.0001. **B.** Empty cecal weight of mixed-sex wild type and CB_1 receptor knockout mice after 2 or 4 weeks of natural microbial recolonization, compared to mice receiving water or continuous Abx treatment. Data presented as mean ± SEM, groups compared with two-way ANOVA followed by Sidak's multiple comparison test, n = 5-13/group. *p < 0.05, **p < 0.01, ***p < 0.001, ****p < 0.0001, †p <0.05 vs wild type mice with same treatment. **C. & D.** Alpha diversity in the gut microbiota measured by Simpson's (**C**) and Shannon's (**D**) diversity indices. Fecal samples of mixed-sex wild type or CB_1 receptor knockout mice with 2 weeks of antibiotic treatment followed by 2 or 4 weeks of natural microbial recolonization were compared to mice receiving water or continuous antibiotic treatment. WT = wild type; CB1KO = CB_1 receptor knockout; Abx = antibiotic treatment; Abx-W = antibiotic withdrawal. Groups analysed with ordinary two-way ANOVA followed by Tukey's multiple comparison test, n = 3-5/group. *p < 0.05, **p < 0.01, ***p < 0.001, ****p < 0.0001. **E.** Fecal microbiota beta diversity (Bray-Curtis index, PCoA) in mixed-sex wild type or CB_1 receptor knockout mice with 2 weeks of antibiotics treatment followed by 2 weeks of natural microbial recolonization, compared to mice receiving water or continuous antibiotics treatment. Circles indicate 80% confidence interval. All time points compared to control with PERMANOVA. Abx WT vs Abx CB1KO: p = 0.121 F = 2.35; AbxW WT vs AbxW CB1KO: p = 0.113 F = 1.90; Con WT vs Con CB1KO: p = 0.086 F = 1.78; Abx vs Con: p = 0.001 F = 41.86; AbxW vs Con: p = 0.001 F = 7.61; Abx vs AbxW: p = 0.001 F = 16.01.

The effects of microbiota depletion and natural microbial recolonization on neurons and enteric glia in the ENS

As expected [14,32], treatment with antibiotics reduced the number of myenteric neurons (HuC/D$^+$ cells) in the ileum (Figure 5A, Supplementary Figure 3A) and colon (Figure 6A, Supplementary Figure 4A). Following antibiotic withdrawal there is a complete recovery of enteric neuronal density, as we have previously published in wild type mice for HuC/D$^+$ neurons and NOS$^+$ neurons [14] (Figures 5A, 5B, Supplementary Figure 3A). This was also the case for the CB_1 receptor knockout mice. Closer examination of the major subtypes of neurons (NOS$^+$ and ChAT$^+$) revealed an identical pattern of loss and recovery in the ileum of both wild type and CB_1 receptor knockout mice (Figures 5B, 5C, Supplementary Figure 3A).

Figure 5

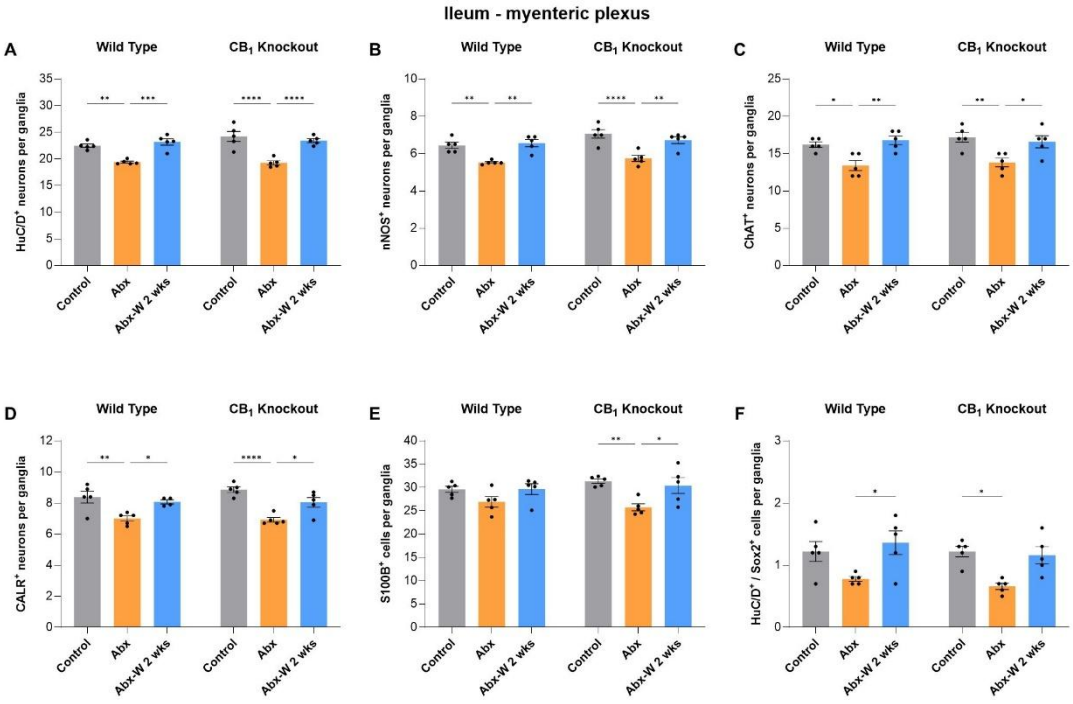

Figure 5. The effects of microbial depletion and natural microbial recolonization on the myenteric plexus of the ileum

Cell density in the myenteric plexus of the ileum of mixed-sex CB_1 knockout mice and wild type control mice treated with water (Control), antibiotic cocktail for 28 days (Abx) or after the natural recolonization 14 days after Abx withdrawal (Abx-W 2 wks). **A.** HuC/D$^+$ neurons per ganglia. **B.** Neuronal nitric oxide synthase (nNOS$^+$) neurons per ganglia. **C.** Choline acetyltransferase (ChAT$^+$) neurons per ganglia. **D.** Calretinin (CALR$^+$) neurons per ganglia. **E.** S100B$^+$ glial cells per ganglia. **F.** HuC/D$^+$ / Sox2$^+$ cells per ganglia. No differences between the two genotypes were observed. Mean ± SEM, groups compared with two-way ANOVA followed by Sidak's multiple comparison test, n = 5/group. *p < 0.05, **p < 0.01, ***p < 0.001, ****p < 0.0001.

Supplementary Figure 3

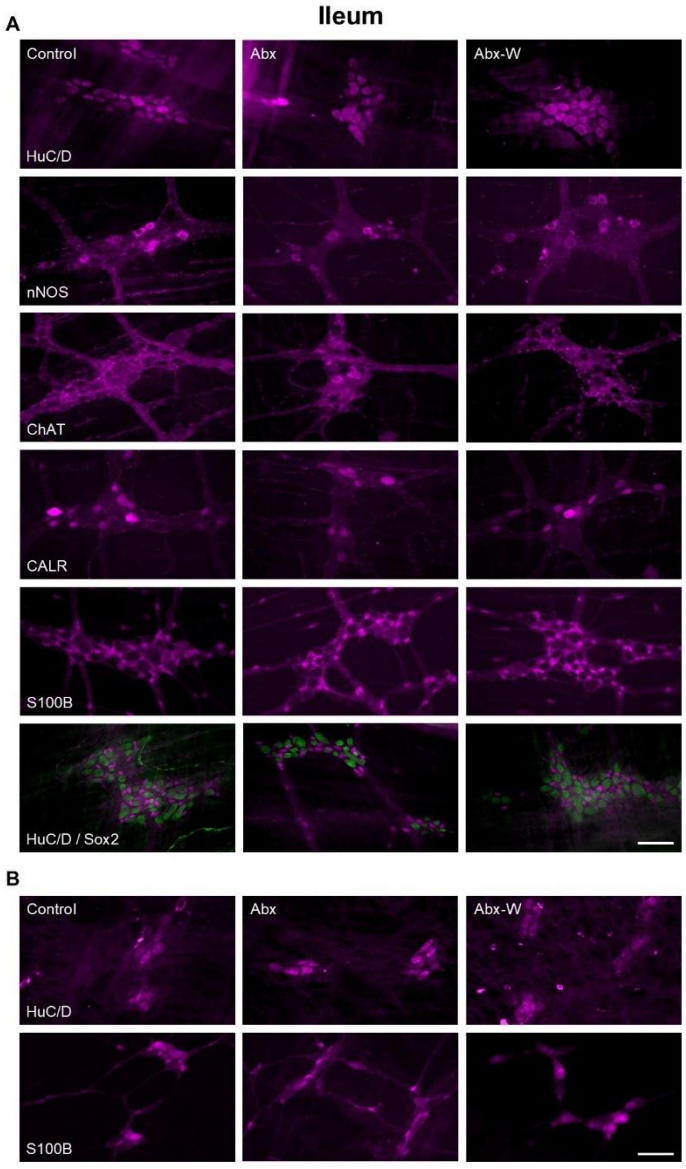

Supplementary Figure 3. ENS changes in the ileum of mice after microbiota depletion and natural recolonization

Representative images of the ENS in the ileum of mixed-sex wild type mice, comparing groups that received water (Control), continuous antibiotics treatment (Abx), or 2 weeks of antibiotics treatment followed by 2 weeks of natural microbial recolonization (Abx-W). Representative images from CB_1 knockout mice are not shown, since the neuronal density per ganglia for each group was identical to the corresponding wild type mice. **A.** Single-labeling

immunofluorescence in the myenteric plexus for HuC/D$^+$ neurons, neuronal nitric oxide synthase (nNOS$^+$) neurons, choline acetyltransferase (ChAT$^+$) neurons, calretinin (CALR$^+$) neurons and S100B$^+$ glial cells. Double-labelling for HuC/D$^+$ neurons (green) and SOX2$^+$ cells (magenta). Scale bar: 30 µm. **B.** Single-labeling immunofluorescence in the submucosal plexus for HuC/D$^+$ neurons and S100B$^+$ glial cells. Scale bar: 15 µm.

In the colon, there was only a small reduction in myenteric neuronal density of NOS$^+$ neurons following treatment with antibiotics that did not reach statistical significance for either wild type or CB_1 receptor knockout mice (Figure 6B, Supplementary Figure 4A), but for ChAT$^+$ neurons, we observed the same pattern as in the ileum in response to antibiotic treatment (Figure 6C, Supplementary Figure 4A). We also evaluated myenteric neurons expressing calretinin (a subpopulation of ChAT$^+$ neurons) and enteric glia expressing S100B in both regions of the gut. Calretinin expression followed the same pattern of reduction and recovery in the ileum but was not affected by antibiotic treatment in the colon of either group of mice (Figures 5D, 6D, Supplementary Figure 3A). S100B$^+$ enteric glia were not significantly altered in the myenteric plexus of the ileum of wild type mice, but in CB_1 receptor knockout mice they were significantly reduced and fully recovered (Figure 5E, Supplementary Figure 3A). In contrast, in the myenteric plexus of the colon, no changes in S100B expression were observed (Figure 6E, Supplementary Figure 4A). Finally, we examined Sox2 expression in neurons of the myenteric plexus of the ileum and colon, as an indicator of enteric neurogenesis [14,34,35]. In the ileum, there was little change in overall Sox2 expression (data not shown), however, the numbers of Sox2$^+$-HuC/D$^+$ neurons were reduced by antibiotic treatment, and they recovered to baseline levels after withdrawal (Figure 5F, Supplementary Figure 3A). In the myenteric plexus of the colon, Sox2$^+$-HuC/D$^+$ neurons were slightly increased in both groups of mice by antibiotic treatment (Figure 6F, Supplementary Figure 4A), as previously reported in wild type animals [14].

In the submucosal plexus of the ileum and colon, as previously reported [14], neuronal density was reduced by antibiotic treatment, and this recovered after antibiotic withdrawal (Figures 7A,

7B, Supplementary Figures 3B, 4B). The same was observed in CB_1 receptor knockout mice. We also examined $S100B^+$ enteric glia, which were essentially not affected by antibiotic treatment in the ileum (Figure 7C, Supplementary Figure 3B). In contrast, in the colonic submucosal plexus of both wild type and CB_1 receptor knockout mice, there was a small, but significant, reduction the $S100B^+$ enteric glia that did not recover upon antibiotic withdrawal (Figure 7D, Supplementary Figure 4B).

Figure 6

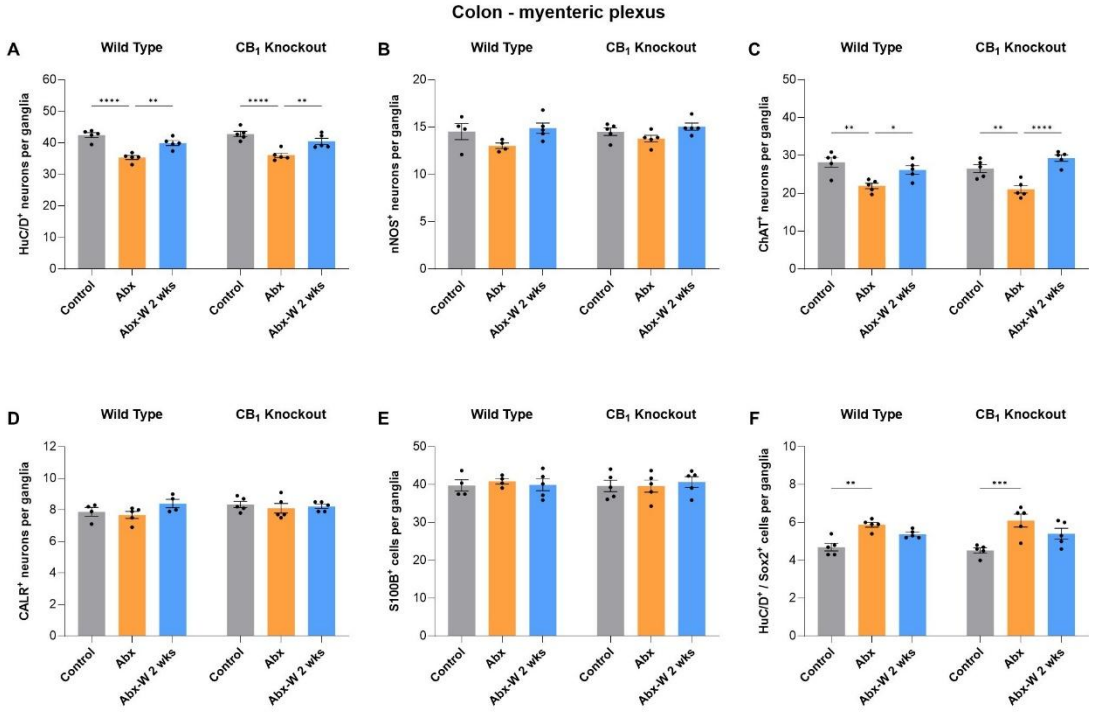

Figure 6. The effects of microbial depletion and natural microbial recolonization on the myenteric plexus of the colon

Cell density in the myenteric plexus of the colon of mixed-sex CB_1 knockout mice and wild type control mice treated with water (Control), antibiotic cocktail for 28 days (Abx) or after the natural recolonization 14 days after Abx withdrawal (Abx-W 2 wks). **A.** HuC/D^+ neurons per ganglia. **B.** Neuronal nitric oxide synthase ($nNOS^+$) neurons per ganglia. **C.** Choline acetyltransferase ($ChAT^+$) neurons per ganglia. **D.** Calretinin ($CALR^+$) neurons per ganglia. **E.** $S100B^+$ glial cells per ganglia. **F.** HuC/D^+ / $Sox2^+$ cells per ganglia. No differences between the two genotypes were observed. Mean ± SEM, groups compared with two-way ANOVA followed by Sidak's multiple comparison test, n = 5/group. *p < 0.05, **p < 0.01, ***p < 0.001, ****p < 0.0001.

Figure 7

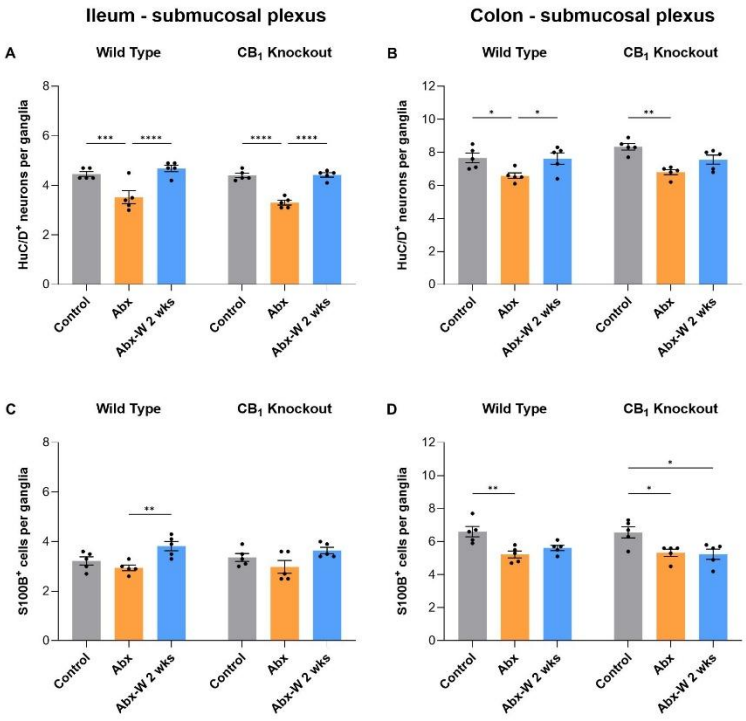

Figure 7. The effects of microbial depletion and natural microbial recolonization on the submucosal plexus of the ileum and colon

Cell density in the submucosal plexus of the ileum and colon of mixed-sex CB_1 knockout mice and wild type control mice treated with water (Control), antibiotic cocktail for 28 days (Abx) or after the natural recolonization 14 days after Abx withdrawal (Abx-W 2 wks). **A. & B.** HuC/D^+ neurons per ganglia in the in the ileum (**A**) and colon (**B**). **C. & D.** $S100B^+$ enteric glial cells per ganglia in the ileum (**C**) and colon (**D**). Mean ± SEM, groups compared with two-way ANOVA followed by Sidak's multiple comparison test, n = 5. *p < 0.05, **p < 0.01, ***p < 0.001, ****p < 0.0001.

Supplementary Figure 4

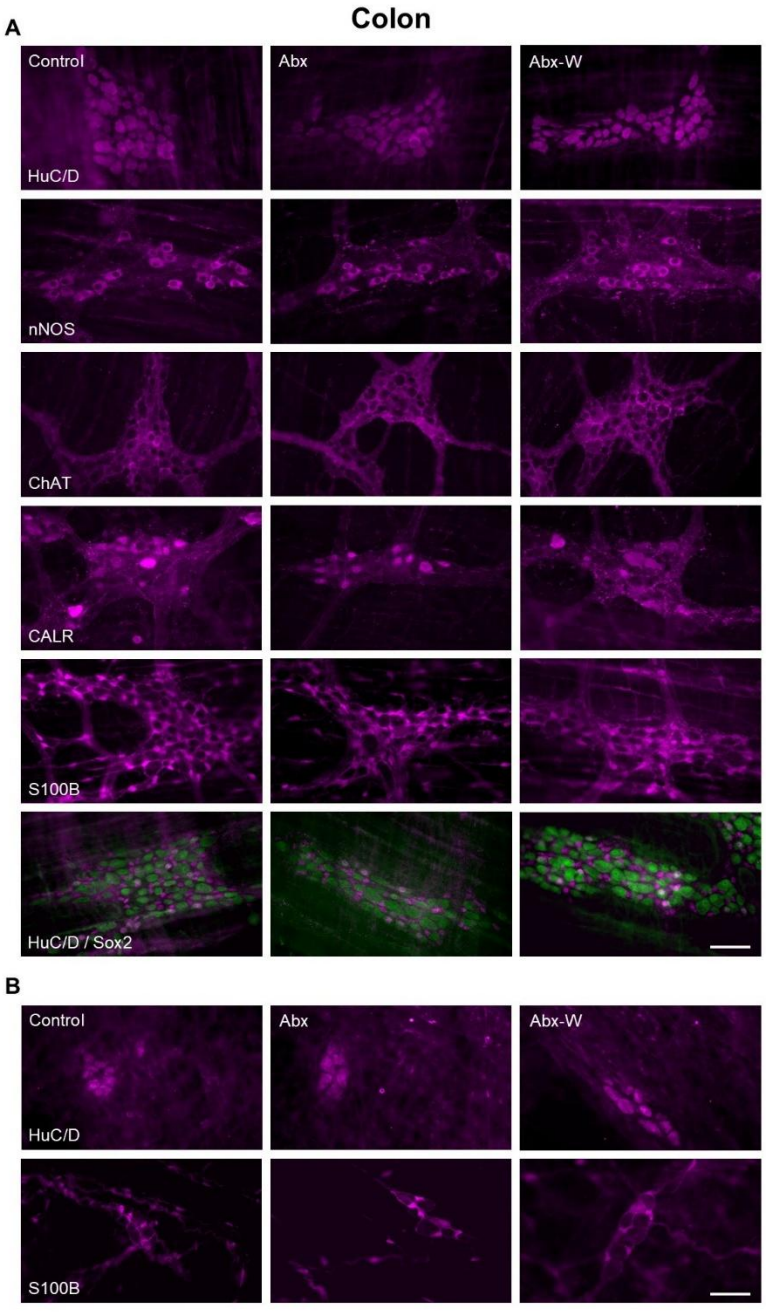

Supplementary Figure 4. ENS changes in the colon of mice after microbiota depletion and natural recolonization

Representative images of the ENS in the colon of mixed-sex wild type mice, comparing groups that received water (Control), continuous antibiotics treatment (Abx), or 2 weeks of antibiotics treatment followed by 2 weeks of natural microbial recolonization (Abx-W). Representative images from CB1 knockout mice are not shown, since the neuronal density per ganglia for each group was identical to the corresponding wild type mice. **A.** Single-labeling immunofluorescence in the myenteric plexus for HuC/D$^+$ neurons, neuronal nitric oxide synthase (nNOS$^+$) neurons, choline acetyltransferase (ChAT$^+$) neurons, calretinin (CALR$^+$) neurons and S100B$^+$ glial cells. Double-labelling for HuC/D$^+$ neurons (green) and SOX2$^+$ cells (magenta). Scale bar: 30 µm. **B.** Single-labeling immunofluorescence in the submucosal plexus for HuC/D$^+$ neurons and S100B$^+$ glial cells. Scale bar: 15 µm.

The effects of microbiota depletion and natural microbial recolonization on GI physiology

We examined intestinal motility, fecal water content as a proxy for colonic secretion, and intestinal barrier function in mixed sex groups of wild type and CB_1 receptor knockout mice. As expected, after antibiotic treatment, whole gut transit time assessed using the passage of Evans Blue dye, was significantly slowed in both groups of mice (Figure 8A). Whole gut transit was significantly faster in CB_1 receptor knockout mice, consistent with the role for CB_1 receptors in regulating gut motility [26,27]. After antibiotic withdrawal, there was only a partial recovery with significantly faster transit in CB_1 receptor knockout mice compared to wild type controls (Figure 8A).

We evaluated small intestinal transit and found that there was a significantly reduced small intestinal transit in both groups of mice after antibiotic treatment that almost fully recovered after antibiotic withdrawal in CB_1 knockout mice, but only partially so in wild type animals (Figure 8B). We did not observe the differential effects between wild type and CB_1 receptor knockout mice that we saw for whole gut transit. Using a bead expulsion assay to assess colonic

motility, we noted that antibiotic treatment had no effect in CB_1 knockout mice but slowed expulsion in wild type mice (Figure 8C). Untreated CB_1 knockout mice also had slower colonic expulsion times than wild type mice (Figure 8C).

We saw no differences in the fecal wet-dry ratio in any of the groups (Figure 8D). Finally, we saw no changes in a marker of intestinal permeability (serum FSA) after antibiotic treatment in wild type or CB_1 receptor knockout mice (Supplementary Figure 5).

Figure 8

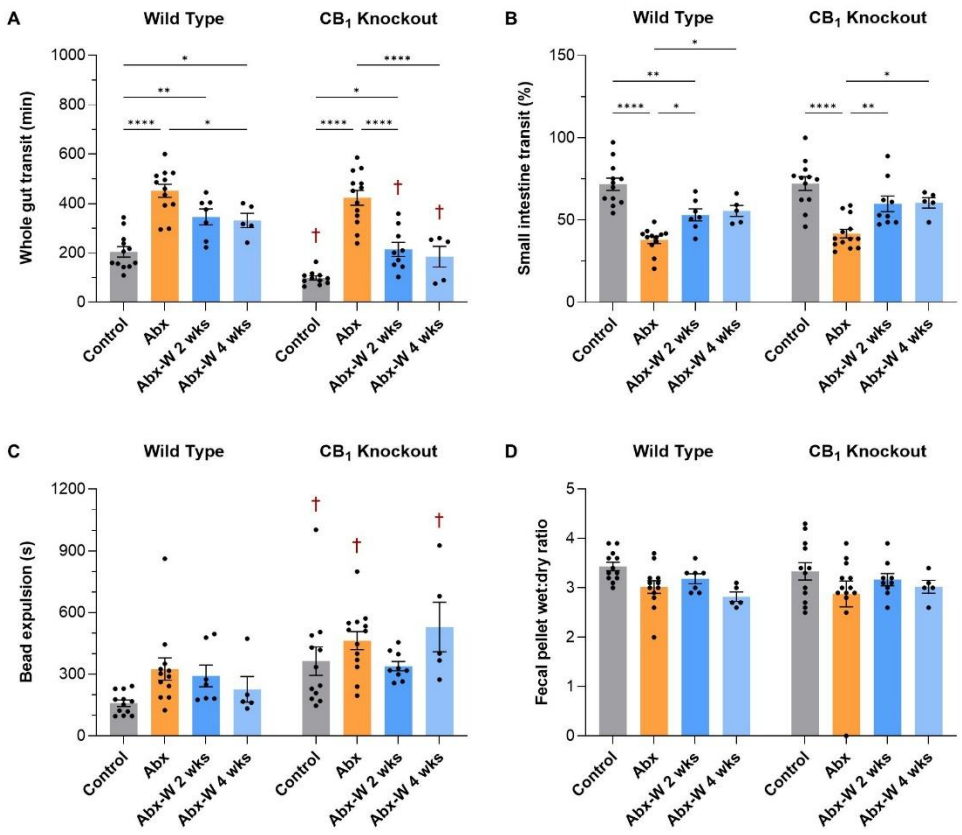

Figure 8. The effects of microbial depletion and natural microbial recolonization on parameters of GI physiology

Assessment of physiological parameters on mixed-sex CB_1 knockout mice and wild type control mice treated with water (Control), antibiotic cocktail for 28 days (Abx) or after the natural recolonization 14 days (Abx-W 2 wks) and 31 days (Abx-W 4 wks) after Abx withdrawal. **A.** Whole gut transit time, measured by marked fecal pellets after gavage with Evan's blue dye. **B.** Small intestine transit, measured by % of small intestine length after gavage with Evan's blue dye. **C.** Distal colonic motility, measured by bead expulsion time. **D.** Fecal pellet wet:dry ratio, measured in feces collected over a 1-hour period. Mean ± SEM, groups compared with two-way ANOVA followed by Sidak's multiple comparison test, n = 5-13. *p < 0.05, **p < 0.01, ***p < 0.001, ****p < 0.0001, †p < 0.05 vs wild type mice with the same treatment.

Supplementary Figure 5

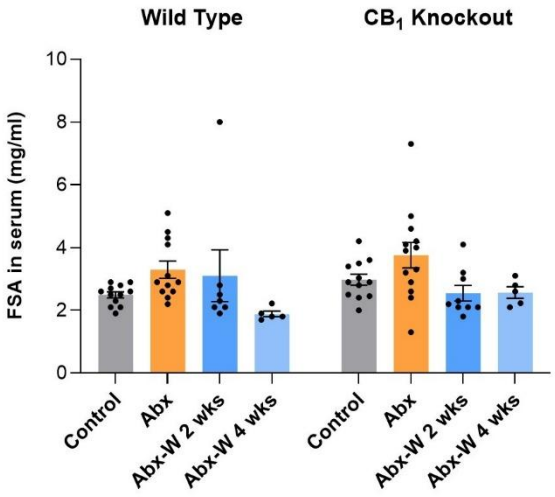

Supplementary Figure 5. Intestinal permeability in mice after microbial depletion and natural recolonization

Assessment of intestinal permeability assessed by fluorescein-5-6-sulfonic acid (FSA) concentration in the serum 4 h after gavage in mixed-sex CB_1 knockout mice and wild type control mice treated with water (Control), antibiotic cocktail for 28 days (Abx) or after the natural recolonization 14 days (Abx-W 2 wks) and 31 days (Abx-W 4 wks) after Abx withdrawal. Mean ± SEM, groups compared with two-way ANOVA followed by Sidak's multiple comparison test, n = 5-13/group. There were no significant differences between any of the groups.

Discussion

There is increasing evidence for interactions between the endocannabinoid system of the GI tract and the gut microbiota [19-25,36,37]. Here we characterized the ENS in CB_1 receptor knockout mice and revealed that the endocannabinoid system signaling is not required for the normal development of the ENS in the small or large intestine, as neuronal and glial density and the major subtypes of enteric neurons were essentially identical between male and female wild type and CB_1 receptor knockout mice. Gut microbiota diversity was affected by antibiotic treatment to a similar extent in both wild type and CB_1 receptor knockout mice, with fecal bacterial load returning to normal levels after two weeks of natural recolonization, and alpha and beta diversity virtually restored to normal levels. CB_1 knockout mice lost more weight on antibiotics than wild type controls. These data add further support to the interaction between the endocannabinoid system and the gut microbiota in the control of body weight and metabolism and are consistent with the literature using CB_1 receptor antagonists [22,24].

When the gut microbiota was depleted by antibiotic treatment, both genotypes had similar physiological changes in the GI tract, such as increased cecal weight, slower whole gut transit and small intestinal transit, fecal pellet water content and intestinal permeability. CB_1 receptor knockout mice differed from wild type mice by having faster whole gut transit time, as previously reported in some [26,38,39], but not all studies [40,41]. This was reduced by antibiotic treatment and was significantly faster in CB_1 knockout mice after initial recolonization. Directly related to the changes in GI physiology, neuronal and glial cell density in the ENS of the ileum and colon generally followed the same pattern in both genotypes: depletion of gut bacteria reduced the cell density, while natural microbiota recolonization restored those populations to normal levels. Importantly, CB_1 receptor knockout mice showed the same neuronal and glial cell density as wild type mice in all populations analysed after antibiotic treatment or natural microbiota recolonization, indicating that endocannabinoid signaling via CB_1 receptors in the ENS is neither protective against neuronal loss, nor essential for neuroregeneration.

Mice treated with a mixture of broad spectrum antibiotics are expected to lose a little weight during the first days of treatment, which can be greatly mitigated by introducing metronidazole gradually instead of at full concentration from the beginning of treatment [14,42]. It was therefore interesting that depletion of the gut microbiota caused a significant weight loss in CB_1 receptor knockout mice despite the gradual introduction of metronidazole, which was rapidly restored after stopping Abx treatment. Mice raised in germ-free conditions and Abx-treated mice have significant changes in the endocannabinoidome, including CB_1 receptors [21,36,43]. We were nevertheless surprised to see such a marked effect in CB_1 receptor knockout mice. Exploring the mechanisms of this finding was beyond the scope of the current study, but this observation further underscores the close linkages between the gut microbiota and endocannabinoid signaling in the GI tract to influence food intake and metabolism [44].

The gut microbiota is essential for normal GI function and ENS integrity, and gut microbiota dysbiosis is related to neuroanatomical and physiological changes in the gut [4,5,45]. Studies from our lab and others have found that mice with antibiotic-depleted gut microbiota or raised under germ free condition have indiscriminate neuronal loss in the both the myenteric plexus and the submucosal plexus [14,33,46-49]. Strikingly, the ENS is capable of recovery in a matter of days after the gut microbiota is restored, suggesting that bacteria and/or their metabolites regulate neuronal and glial structure and function, modulating gut physiology. Although the exact mechanisms are still unknown, activation of TLR2 and TLR4 by bacterial molecules enhances neuronal survival and neuroregeneration [14,50,51]. Since cannabinoids interact with TLR signalling in various cell types [52-54], we investigated in this study if CB_1 receptors are involved in the physiological recovery of the ENS and GI motility in response to natural microbial recolonization.

Before the experiments with gut microbiota depletion and recolonization, we first characterized the ENS of CB_1 receptor knockout mice. Compared to wild type mice, CB_1 receptor knockout male or female mice showed no differences in neuronal or glial cell density or any of the major populations of enteric neurons we analyzed in the ileum and colon, both in

the myenteric or submucosal plexuses. In the CNS, CB_1 signaling is important for adult neurogenesis [55] as well as for establishing the normal density and connectivity of neurons in the striatum [56,57] and in neuronal structure in other brain regions [58,59]. Whilst we only examined the total neuronal and enteric glial cell density and the major populations of neurochemically coded subtypes of enteric neurons, our results suggest potential differences between the CNS and ENS in the role of CB_1 receptors for the development of the ENS. Alternatively, since our mice were a global embryonic knockout, we may be observing the ability of the ENS to compensate for the loss of this receptor. Further studies are needed to examine these two possibilities.

Using Sox2 as a marker for evaluating glia-to-neuron differentiation [14,34,35], we found regional differences in the density of $Sox2^+$ neurons in the myenteric plexus of Abx-treated mice from both genotypes: reduced density in the ileum, which recovered to baseline after natural microbiota recolonization, and increased density in the colon, which remained slightly increased after recolonization. These results imply that the ENS in distinct areas of the GI tract may respond differently to the same environmental disturbances depending on their physiological function. This was especially interesting for the Abx-treated mice, considering that the colon did not show the same neuronal loss in all subpopulations that we observed in the ileum. It is possible that the faster rate of neurogenesis observed in the colon with the depletion of gut microbiota was sufficient to maintain some of those neuronal populations. Nevertheless, the myenteric neurogenesis we observed in the natural microbiota recolonization group was consistent with the recovery in neuronal density for the affected populations and was similar in both genotypes of mice.

One of the main roles of the endocannabinoid system in GI homeostasis is the regulation of gut motility [15,27]. CB_1 receptors are found in neurons and nerve fibers of both the myenteric and submucosal plexuses [26,60-62], and their activation by endocannabinoids inhibits the release of neurotransmitters at enteric synapses, slowing down gut motility in normal physiological conditions [26]. Less is known about the exact role of enteric glia in endocannabinoid signaling in

the ENS; although glial cells show limited expression of cannabinoid receptors [18,63], they are the primary site of monoacylglycerol lipase expression in the ENS [18], the enzyme that hydrolyses 2-AG. Since this is a key enzyme in endocannabinoid signaling, glial cells seem to play a significant role in the control that the endocannabinoid system exerts in the ENS. Our results indicate that endocannabinoid signaling via CB_1 receptors, or the lack of signaling thereof, have no influence in the normal development and the structure of the ENS, and this is independent of sex. This also implies that the faster GI transit observed in CB_1 knockout mice is a direct physiological consequence of the inhibition of the endocannabinoid tone in gut, rather than a neuroanatomical change in the density and composition of the ENS.

The GI physiology experiments presented in this paper showed that CB_1 knockout mice follow the same pattern of dysmotility/recovery observed in wild type mice, when treated with Abx followed by natural gut microbiota recolonization. Untreated CB_1 knockout mice had faster whole gut transit than wild type mice and following natural microbiota recolonization there was full recovery to normal motility. These findings are consistent with the inhibitory role of CB_1 receptors [26,61,64] despite that both genotypes had their GI transit slowed to the same levels when gut microbiota was depleted by Abx. Since we observed a similar loss of neurons in both genotypes of mice with Abx treatment these data suggest that the physiological changes resulting from neuronal loss are significant enough to overcome the naturally faster GI motility mediated by the lack of the endocannabinoid tone in CB_1 knockout mice, and it also reveals how impactful the depletion of gut microbiota is to the ENS and gut motility. Despite the Abx treatment not affecting distal colonic motility, CB_1 knockout mice had slower overall colonic motility than wild type mice. This was unexpected based on the literature where it was not previously observed [62]. Considering that the loss of the endocannabinoid tone should accelerate GI motility it is also surprising, but previous studies in CB_1 receptor knockout mice and using CB_1 receptor antagonists reveal no increases in colonic motility [60,62], despite the fact that CB_1 receptor agonists powerfully slow the colon [39,62]. Since endocannabinoids can also interact with receptors other than canonical CB receptors, such as TRPV1 [15], and due to the mechanical distension of the bead expulsion test, it is possible that other signaling pathways

involving sensory innervation of the ENS could be affecting the slower colonic transit in CB_1 knockout mice. Further studies are required to examine this finding.

Changes in GI motility were likely a result of the indiscriminate neuronal loss observed in the myenteric plexus, rather than changes in one specific neuronal circuit component (excitatory, inhibitory or inter neurons). This was especially true in the ileum, where all neuronal populations lost neurons with microbiota depletion and recovered back to baseline after natural recolonization, while the colon had significant changes mainly in excitatory neurons ($ChAT^+$ cells). Our study also expands these findings by showing that the endocannabinoid signaling via CB_1 receptors does not seem to have any influence in mitigating the ENS neuronal loss or neurogenesis, as the neuronal density for all populations analyzed were essentially identical between wild type and CB_1 receptor knockout mice.

In conclusion, this study reveals new insights into the interaction between the gut microbiota and endocannabinoid system of the GI tract. Previous studies have shown that a deficiency of cannabinoid receptor signaling enhances the susceptibility to bacterial infection [65] and germ free mice have altered CB_1 receptor expression throughout the GI tract [21]. Together these suggested a role for endocannabinoid-microbiota cross talk in the regulation of the gut function. We used Abx treatment as way to perturb the gut microbiota in adult animals, and whilst subject to limitations, is a convenient way to examine neuroanatomical and physiological changes to the gut. Since CB_1 receptors are the dominant CB receptor in the gut, we examined how mice lacking these receptors would respond to Abx treatment. There were relatively few differences between the genotypes of mice observed in these studies, with no differences in the response of the ENS to microbial depletion and recolonization. The main functional differences we noted were that Abx-treated CB_1 receptor knockout mice had greater weight loss, faster whole gut transit, but slower colonic motility than wild type animals (that was not perturbed by Abx treatment). Why the CB_1 receptor knockout mice lose more weight and have slower colonic motility remain to be determined. The faster whole gut transit is consistent with an endocannabinoid tone in the small intestine. Future studies that examine the role of

endocannabinoid signalling in the control of gut physiology in conditions of microbial dysbiosis will further extend insights into the endocannabinoid-microbiota cross talk in the GI tract.

Acknowledgements

The authors thank Dr. Fernando Vicentini for valuable discussion and the International Microbiome Centre, University of Calgary for technical support.

Funding

This work was supported by a grant from the Canadian Institutes of Health Research to KAS (FDN148380). YBH is the recipient of a TRIANGLE Canada fellowship award.

Conflict of interest

The authors declare they have no conflicts of interest.

Author contributions

EB, YBH and KAS designed the studies; EB, YBH, CMK and LEW conducted experiments and performed data analyses; EB, YBH and KAS drafted the manuscript. All authors had access to the study data and critically reviewed manuscripts drafts and approved the final manuscript for submission. KAS obtained funding for the study and provided study supervision.

Materials and Methods

Animals

Male and female CB_1 knockout (C57BL/6 background) mice and wild-type littermates (bred in house), 8-12 weeks old, were used in this study [26,66]. Mice were kept in a room under a 12 h light-dark cycle, with controlled temperature and humidity conditions, and were acclimatized to the housing facility for at least 7 days before the experiment start. Mice were group housed (up to 5 mice per cage) and had free access to sterilized food and water throughout the experiment. Euthanasia was performed by cervical dislocation under isoflurane anesthesia (5% in oxygen). All animal procedures were approved by the University of Calgary Health Sciences Animal Care Committee (#AC19-0124, AC23-1035) and were conducted in accordance with the guidelines established by the Canadian Council on Animal Care.

Broad-spectrum antibiotic treatment

Broad-spectrum antibiotic (Abx) treatment was administered according to previously published protocols [14], where mice received an Abx solution in drinking water for 14, 28, or 45 days (Figure 3). The Abx mix was diluted in sterilized water and consisted of ampicillin (1 g/L, Sigma-Aldrich), neomycin (1 g/L, Sigma-Aldrich, St. Louis, MO, USA), vancomycin (0.5 g/L, Sigma-Aldrich), and metronidazole (1 g/ L, Sigma-Aldrich). Due to the initial body weight loss caused by the Abx treatment (PMID: 21445311), metronidazole was gradually introduced in the Abx solution as previously described [14]: no metronidazole added on day 0; 0.25 g/L (25% of final concentration) added at day 2; 0.5 g/L (50% of final concentration) added at day 6; and 1.0 g/L (full concentration) added at day 9. Body weight was assessed three times a week to monitor body weight changes, and the Abx solution was changed every week. In the two groups where we assessed the effects of spontaneous microbiota recolonization, the bottles of Abx were swapped for regular autoclaved water at day 14. Mice had access to regular water for another 14 or 31 days after this to allow for microbiota recolonization.

In vivo measurements of GI motility

The GI motility tests were performed during the last week of the study, as shown in Figure 3A. Mice were allowed to rest for 4 days between the whole gut transit, distal colonic transit, and small intestine transit tests. Because there was no difference in the physiological parameters measured in the control and Abx-treated groups when comparing the experiments with 14 days versus 31 days of natural microbiota recolonization, we opted to merge the data presented for those two groups.

Whole gut transit and fecal water content

To measure whole gut transit time, mice were gavaged with 200 µL of the non-absorbable dye Evans Blue (5% suspended in 5% Gum Arabic; Sigma-Aldrich) and placed in individual, bedding-free cages. The period from the time of the gavage to the appearance of the first blue colored fecal pellet was considered the whole gut transit time, with a maximum waiting time of 600 min. Fecal water content was assessed by the fecal pellet wet:dry ratio. During the first hour after the dye gavage, fecal pellets were collected and weighed every 15 min. Feces were dried at 50°C for 24 h and re-weighed to generate the wet:dry ratio.

Small intestinal transit

Mice were gavaged with 200 µL of the non-absorbable dye Evans Blue and euthanized under isoflurane anesthesia after 15 min. The small intestine was fully removed (pyloric sphincter to ileal–cecal junction) and its length measured, as well as the distance traveled by the dye. Results are expressed as a percentage of the total small intestinal length covered by the dye. This test was performed in parallel with the intestinal permeability assay (see below); mice received the Evans Blue gavage 3 h 45 min after the start of the intestinal permeability assay.

Colonic bead expulsion

Colonic propulsion was assessed by the bead expulsion test. Mice were lightly anesthetized with isoflurane (2% in oxygen) and a 2.5 mm spherical plastic bead was gently inserted 2 cm into the distal colon using a silicone pusher. Mice recovered in < 1 min after insertion of the

bead and were placed in individual, bedding-free cages, and latency time for bead expulsion was recorded. Experiments were repeated 3 times with 100 min intervals, and mice were returned to their home cage between the repetitions. The mean of 3 repetitions was recorded as time for bead expulsion.

Intestinal permeability assay

Mice were gavaged with 100 µL of fluorescein-5(6)-sulfonic acid ((FSA) 50 mg/mL; Setareh Biotech, Eugene, OR, USA) and anesthetized under isoflurane after 4 h. Blood was drawn by cardiac puncture and collected in a Microtainer SST Tube (BD Biosciences, Mississauga, ON, Canada), after which mice were euthanized for tissue collection. Blood was allowed to clot for at least 30 min at room temperature, followed by centrifugation at 2000 × g for 10 min. The supernatant (serum) was collected, pipetted (50 µL) in triplicate into a 96-well plate, and read at 485/535 nm in a spectrophotometer. Sample FSA concentration (µg/mL of serum) was determined using a standard curve.

Tissue collection

After *in vivo* experiments, mice were deeply anesthetized with isoflurane (5% in oxygen) and euthanized by cervical dislocation. The entire gut was removed, and the length of the small intestine and colon was measured. For the Abx experiments, the full cecum was weighed, and a portion of the cecal contents was collected and immediately frozen in dry ice for the fecal bacteria load and microbiota analysis. Cecal contents were then removed, and the empty cecum was weighed again.

Whole-mount preparations

The ileum and colon were processed and dissected as previously described [14]. The distal segment of the ileum and the proximal segment of the colon (6 cm each) were first bathed for 10 min in a solution containing 1 µM nifedipine (Sigma-Aldrich) diluted in ice-cold phosphate-buffered saline (PBS). Tissues were opened along the mesenteric border, their contents cleaned with PBS, and they were pinned out with the serosal side facing down in a Petri dish coated

with Sylgard (Dow Silicones Corp, Midland, MI, USA). Samples were fixed with either Zamboni's fixative for 24 h at 4°C (for most of the antibodies), or with 4% paraformaldehyde (ThermoFisher Scientific, Waltham, MA, USA) for 2 h at 4°C (for ChAT antibodies). Tissues were then washed (3 times, 10 min each) with PBS containing 0.05% sodium azide (EM Science, Hatfield, PA, USA) and stored at 4°C until further processing. Whole-mount preparations of the myenteric and submucosal plexus were dissected under a microscope. Myenteric plexus preparations were acquired by stripping off the mucosa/submucosa layers and the circular muscle, leaving a preparation consisting of the longitudinal muscle and associated myenteric plexus. Submucosal plexus preparations were obtained by gently scraping the mucosa away and peeling off the submucosal plexus.

Immunofluorescence labelling of the ENS

Dissected whole-mount preparations were first washed (3 times, 5 min each) in PBS containing 0.1% Triton X-100 (Sigma-Aldrich (PBS+T)) and incubated with primary antibody for 48 h at 4°C (Table 1). The primary antibody solution was removed, and samples were washed (3 times, 5 min each) with PBS+T, followed by incubation with secondary antibody (Table 1) for 2 h at room temperature. The secondary antibody solution was then removed, samples were washed (3 times, 5 min each) with PBS and mounted with bicarbonate-buffered glycerol on microscope slides, stored at 4°C under dark conditions. For double-labeled whole-mounts, the second labeling was performed by following the same protocol immediately after the first labeling. Immunofluorescence labeling of different enteric populations was done similarly for the ileum and colon, with minor changes for specific antibodies. When using anti-Sox2 antibodies, samples were pre-treated with dimethyl sulfoxide (Sigma Aldrich) for 30 min at room temperature prior to primary antibody incubation. In the same way, samples labeled with anti-ChAT antibodies were pre-treated with methanol for 30 min at -20°C. All antibodies used were diluted in a PBS+T solution containing 10% bovine serum albumin (Sigma-Aldrich), 0.05% sodium azide, 0.04% EDTA (Sigma-Aldrich).

TABLE 1. Antibodies used for immunofluorescence labelling of the ENS

Antibody	Dilution	Source	Identifier
Mouse anti-HuC/D	1:200	Invitrogen	Cat# A21271; RRID: AB_221448
Sheep anti-nNOS	1:200	Millipore	Cat# AB1529; RRID: AB_90743
Goat anti-Sox2	1:200	R&D Systems	Cat# AF2018; RRID: AB_355110
Goat anti-ChAT	1:50	Millipore	Cat# AB144P; RRID: AB_2079751
Goat anti-Calretinin	1:200	Swant	Cat# CG1; RRID: AB_10000342
Rabbit anti-S100B	1:500	Agilent Dako	Cat# Z0311; RRID: AB_10013383
Donkey anti-mouse AF488	1:200	Jackson ImmunoResearch	Cat# 715-546-151; RRID: AB_2340850
Donkey anti-sheep CY3	1:100	Jackson ImmunoResearch	Cat# 713-165-147; RRID: AB_2315778
Donkey anti-goat CY3	1:200	Jackson ImmunoResearch	Cat# 705-165-147; RRID: AB_2307351
Donkey anti-rabbit CY3	1:200	Jackson ImmunoResearch	Cat# 711-165-152; RRID: AB_2307443

Quantification of enteric neurons and glial cells

Immunolabelled neurons (HuC/D$^+$, nNOS$^+$, ChAT$^+$, Calretinin$^+$, Sox2$^+$) and glial cells (S100B$^+$, Sox2$^+$) were quantified the same way in both the ileum and colon. Slides were analyzed using a Zeiss Axioplan fluorescence microscope (Zeiss Canada, North York, ON, Canada) and images were captured with a QImaging Retiga-2000R digital monochrome camera (Teledyne Photometrics, Tucson, AZ, USA). For cells counts, 15 ganglia were randomly selected from the images for each preparation, and immunolabelled cells were quantified using the ImageJ software (NIH). Data for each animal is presented as mean number of cells in the 15 ganglia counted. For the natural microbiota recolonization study, all the ENS quantitative analyses were performed in samples from the experiment with 14 days of natural microbiota recolonization.

Quantification of fecal bacterial load

To evaluate the efficacy of Abx treatment and recovery of gut microbiota after Abx withdrawal, cecal samples were collected in a sterile tube after euthanasia and immediately stored in dry ice, followed by -80°C until analysis. DNA was extracted using a DNeasy PowerSoil kit (Qiagen, Hilden, Germany) according to the manufacturer's instructions, with minor modifications. Briefly, samples were homogenized in TissueLyzer LT (Qiagen, Germantown, MD, USA) using 30 Hz for 2x 5min eluted in Tris Buffer (CD6) from the kit. DNA load was quantified using NanoDrop (ThermoFisher Scientific, Wilmington, DE, USA) and standardized to 1 ng/µL in all samples. A qPCR reaction was performed using PerfeCTa SYBR Green SuperMix (QuantaBio, Beverly, MA, USA), with universal bacterial primers UniF340 and UniR514 (PMID: 18160481) used to amplify bacterial DNA. The qPCR mixture solution consisted of 10 µL reactions containing: 5 µL of master mix, 0.5 µL of 5 mM UniF340, 0.5 µL of 5 mM UniR514, 4 µL of DNA sample diluted in nuclease-free water, normalized to 100 ng. The qPCR thermocycler StepOnePlus (Applied Biosystems, Foster City, CA, USA) was set for an initial step at 95 °C for 3 min, followed by 40 cycles of 10 s at 95°C and 30 s at 55°C, with a final step for the melting curve 10 s at 95°C, 5 s at 65°C with a 0.5°C incremental ramp up to 95°C. CT values were acquired in the final step at 55°C, and a melting curve was acquired at the end of the run.

Microbiota sequencing and analysis

Microbiota sequencing and analysis was performed as previously described [67,68]. Bacterial composition was evaluated using 16s rRNA gene amplicon sequencing. Fecal pellets were freshly collected from mice at day 0, 4 weeks and 6 weeks after the start of the study. Upon defecation, 2–3 pellets were immediately collected into sterile microcentrifuge tubes and placed on ice. Bacterial DNA was isolated from samples using the QIAamp PowerFecal Pro DNA Kit (QIAGEN; Hilden, Germany). The V4 hypervariable region of the bacterial 16S rRNA gene was amplified using the following barcoded primers (Integrated DNA Technologies; Coralville, IA, USA):

16SV4Fwd: AATGATACGGCGACCACCGA

BARCODE TATGGTAATTGTGTGCCAGCMGCCGCGGTAA

16SV4Rev: CAAGCAGAAGACGGCATACGAGAT

BARCODE AGTCAGTCAGCCGGACTACHVGGGTWTCTAAT

Using KAPA HiFi polymerase (Roche; Indianapolis, IN, USA) for the reactions, the following cycling conditions used: initial denaturation at 98°C for 2 min, 25 cycles at 98°C for 30 seconds, annealing at 55°C for 30 seconds, extension at 72°C for 20 seconds, and final elongation at 72°C for 7 min. Individual PCR libraries were pooled after amplification, and each sample concentration was measured (Qubit fluorometer, Thermo Fisher Scientific; Waltham, MA, USA). Using a V2-500 cycle cartridge on the MiSeq platform (Illumina; San Diego, CA, USA), the 16S rRNA V4 gene amplicon sequencing was performed. Raw fastq files were then processed with the DADA2 pipeline 1.16 (R package, v1.30.0) and the quality profiles of the forward and reverse reads were visualized. Reads were trimmed to remove the V4 primer regions and the lower quality reads. An amplicon sequence variant (ASV) table was generated after merging the forward and reverse reads. Taxonomic classification was then assigned to each ASV using SILVA ribosomal gene database project (v138.1). Following amplification, individual PCR libraries were pooled, and the concentration of each sample was measured using a Qubit fluorometer (Thermo Fisher Scientific). The 16s rRNA V4 gene amplicon sequencing was performed with a V2-500 cycle cartridge on the MiSeq platform (Illumina; San Diego, CA, USA). The raw fastq files were processed with the DADA2 pipeline 1.16 (R package, version 1.30.0). The quality profiles of the forward and reverse reads were visualized, and the reads were trimmed to remove the V4 primer regions and lower-quality reads. The forward and reverse reads were then merged, and an amplicon sequence variant table (ASV) table was generated. Next, a taxonomic classification was assigned to each ASV using the SILVA ribosomal RNA gene database project (version 138.1) [69]. Afterwards, using DADA2 outputs (R package, v1.46.0), the phyloseq object was created and was used for all downstream analysis.

Statistics

Statistical analyses were performed with GraphPad Prism (GraphPad Software, Boston, MA, USA), and data is presented as mean ± standard error of the mean (SEM). For the CB_1 knockout ENS characterization experiments, comparisons between two groups were performed using unpaired student's t test. For the Abx experiments, analyses were done with Two-way ANOVA followed by Sidak's multiple comparison test. The specific statistical test used in each figure is described in the figure legends, as well as the *n* for each experimental group. $p < 0.05$ was accepted as statistically significant.

For microbiota analysis, alpha diversity was measured using the Shannon and Simpson diversity index, and beta diversity was analyzed using the Bray–Curtis dissimilarity matrix. The Bray–Curtis dissimilarity matrix was visualized using a principal coordinate analysis (PCoA) plot. Ordinary two-way ANOVA followed by Tukey's multiple comparisons test was used for alpha diversity, and PERMANOVA for beta diversity.

References

1. Cho, I. & Blaser, M. J. The human microbiome: at the interface of health and disease. *Nat Rev Genet* **13**, 260-270, (2012).
2. Clemente, J. C., Ursell, L. K., Parfrey, L. W. & Knight, R. The impact of the gut microbiota on human health: an integrative view. *Cell* **148**, 1258-1270, (2012).
3. Cryan, J. F. *et al.* The Microbiota-Gut-Brain Axis. *Physiol Rev* **99**, 1877-2013, (2019).
4. Ghosh, S., Whitley, C. S., Haribabu, B. & Jala, V. R. Regulation of Intestinal Barrier Function by Microbial Metabolites. *Cell Mol Gastroenterol Hepatol* **11**, 1463-1482, (2021).
5. Sharkey, K. A. & Mawe, G. M. The enteric nervous system. *Physiol Rev* **103**, 1487-1564, (2023).
6. Margolis, K. G., Cryan, J. F. & Mayer, E. A. The Microbiota-Gut-Brain Axis: From Motility to Mood. *Gastroenterology* **160**, 1486-1501, (2021).
7. Vicentini, F. A. *et al.* New Concepts of the Interplay Between the Gut Microbiota and the Enteric Nervous System in the Control of Motility. *Adv Exp Med Biol* **1383**, 55-69, (2022).
8. Rooks, M. G. & Garrett, W. S. Gut microbiota, metabolites and host immunity. *Nat Rev Immunol* **16**, 341-352, (2016).
9. Sanz, Y. *et al.* The gut microbiome connects nutrition and human health. *Nat Rev Gastroenterol Hepatol* **22**, 534-555, (2025).
10. Van Hul, M. & Cani, P. D. From microbiome to metabolism: Bridging a two-decade translational gap. *Cell Metab* **38**, 14-32, (2026).
11. Zheng, D., Liwinski, T. & Elinav, E. Interaction between microbiota and immunity in health and disease. *Cell Res* **30**, 492-506, (2020).
12. de Vos, W. M., Tilg, H., Van Hul, M. & Cani, P. D. Gut microbiome and health: mechanistic insights. *Gut* **71**, 1020-1032, (2022).
13. Griffiths, J. A. *et al.* Peripheral neuronal activation shapes the microbiome and alters gut physiology. *Cell Rep* **43**, 113953, (2024).
14. Vicentini, F. A. *et al.* Intestinal microbiota shapes gut physiology and regulates enteric neurons and glia. *Microbiome* **9**, 210, (2021).

15. Cuddihey, H., MacNaughton, W. K. & Sharkey, K. A. Role of the Endocannabinoid System in the Regulation of Intestinal Homeostasis. *Cell Mol Gastroenterol Hepatol* **14**, 947-963, (2022).
16. Di Marzo, V. & Piscitelli, F. Gut feelings about the endocannabinoid system. *Neurogastroenterol Motil* **23**, 391-398, (2011).
17. DiPatrizio, N. V. Endocannabinoids in the Gut. *Cannabis Cannabinoid Res* **1**, 67-77, (2016).
18. Morales-Soto, W., Thomasi, B. & Gulbransen, B. D. Endocannabinoids regulate enteric neuron-glia networks and visceral hypersensitivity following inflammation through a glial-dependent mechanism. *Glia* **72**, 2095-2114, (2024).
19. Cheng, J., Venkatesh, S., Ke, K., Barratt, M. J. & Gordon, J. I. A human gut Faecalibacterium prausnitzii fatty acid amide hydrolase. *Science* **386**, eado6828, (2024).
20. Dohnalova, L. *et al.* A microbiome-dependent gut-brain pathway regulates motivation for exercise. *Nature* **612**, 739-747, (2022).
21. Manca, C. *et al.* Germ-free mice exhibit profound gut microbiota-dependent alterations of intestinal endocannabinoidome signaling. *J Lipid Res* **61**, 70-85, (2020).
22. Mehrpouya-Bahrami, P. *et al.* Blockade of CB1 cannabinoid receptor alters gut microbiota and attenuates inflammation and diet-induced obesity. *Sci Rep* **7**, 15645, (2017).
23. Cani, P. D. *et al.* Endocannabinoids--at the crossroads between the gut microbiota and host metabolism. *Nat Rev Endocrinol* **12**, 133-143, (2016).
24. Muccioli, G. G. *et al.* The endocannabinoid system links gut microbiota to adipogenesis. *Mol Syst Biol* **6**, 392, (2010).
25. Everard, A. *et al.* Intestinal epithelial N-acylphosphatidylethanolamine phospholipase D links dietary fat to metabolic adaptations in obesity and steatosis. *Nat Commun* **10**, 457, (2019).
26. Hons, I. M. *et al.* Plasticity of mouse enteric synapses mediated through endocannabinoid and purinergic signaling. *Neurogastroenterol Motil* **24**, e113-124, (2012).

27. Izzo, A. A. & Sharkey, K. A. Cannabinoids and the gut: new developments and emerging concepts. *Pharmacol Ther* **126**, 21-38, (2010).
28. Berghuis, P. *et al.* Hardwiring the brain: endocannabinoids shape neuronal connectivity. *Science* **316**, 1212-1216, (2007).
29. Maccarrone, M., Guzman, M., Mackie, K., Doherty, P. & Harkany, T. Programming of neural cells by (endo)cannabinoids: from physiological rules to emerging therapies. *Nat Rev Neurosci* **15**, 786-801, (2014).
30. Poon, S. S. B. *et al.* Neonatal antibiotics have long term sex-dependent effects on the enteric nervous system. *J Physiol* **600**, 4303-4323, (2022).
31. Delungahawatta, T. *et al.* Antibiotic Driven Changes in Gut Motility Suggest Direct Modulation of Enteric Nervous System. *Front Neurosci* **11**, 588, (2017).
32. Muller, P. A. *et al.* Microbiota-modulated CART(+) enteric neurons autonomously regulate blood glucose. *Science* **370**, 314-321, (2020).
33. Obata, Y. *et al.* Neuronal programming by microbiota regulates intestinal physiology. *Nature* **578**, 284-289, (2020).
34. Belkind-Gerson, J. *et al.* Colitis promotes neuronal differentiation of Sox2+ and PLP1+ enteric cells. *Sci Rep* **7**, 2525, (2017).
35. Belkind-Gerson, J. *et al.* Colitis induces enteric neurogenesis through a 5-HT4-dependent mechanism. *Inflamm Bowel Dis* **21**, 870-878, (2015).
36. Guida, F. *et al.* Antibiotic-induced microbiota perturbation causes gut endocannabinoidome changes, hippocampal neuroglial reorganization and depression in mice. *Brain Behav Immun* **67**, 230-245, (2018).
37. Dione, N. *et al.* Mgll Knockout Mouse Resistance to Diet-Induced Dysmetabolism Is Associated with Altered Gut Microbiota. *Cells* **9**, (2020).
38. Cluny, N. L. *et al.* Naphthalen-1-yl-(4-pentyloxynaphthalen-1-yl)methanone (SAB378), a peripherally restricted cannabinoid CB1/CB2 receptor agonist, inhibits gastrointestinal motility but has no effect on experimental colitis in mice. *J Pharmacol Exp Ther* **334**, 973-980, (2010).

39. Bashashati, M. *et al.* Inhibiting endocannabinoid biosynthesis: a novel approach to the treatment of constipation. *Br J Pharmacol* **172**, 3099-3111, (2015).
40. Carai, M. A. *et al.* Investigation on the relationship between cannabinoid CB1 and opioid receptors in gastrointestinal motility in mice. *Br J Pharmacol* **148**, 1043-1050, (2006).
41. Taschler, U. *et al.* Monoglyceride lipase deficiency causes desensitization of intestinal cannabinoid receptor type 1 and increased colonic mu-opioid receptor sensitivity. *Br J Pharmacol* **172**, 4419-4429, (2015).
42. Miller, K. A., Vicentini, F. A., Hirota, S. A., Sharkey, K. A. & Wieser, M. E. Antibiotic treatment affects the expression levels of copper transporters and the isotopic composition of copper in the colon of mice. *Proc Natl Acad Sci U S A* **116**, 5955-5960, (2019).
43. Silvestri, C. & Di Marzo, V. The Gut Microbiome-Endocannabinoidome Axis: A New Way of Controlling Metabolism, Inflammation, and Behavior. *Function (Oxf)* **4**, zqad003, (2023).
44. DiPatrizio, N. V. Endocannabinoids and the Gut-Brain Control of Food Intake and Obesity. *Nutrients* **13**, (2021).
45. Ohara, T. E. & Hsiao, E. Y. Microbiota-neuroepithelial signalling across the gut-brain axis. *Nat Rev Microbiol* **23**, 371-384, (2025).
46. Caputi, V. *et al.* Antibiotic-induced dysbiosis of the microbiota impairs gut neuromuscular function in juvenile mice. *Br J Pharmacol* **174**, 3623-3639, (2017).
47. Bernabe, G. *et al.* Antibiotic Treatment Induces Long-Lasting Effects on Gut Microbiota and the Enteric Nervous System in Mice. *Antibiotics (Basel)* **12**, (2023).
48. Collins, J., Borojevic, R., Verdu, E. F., Huizinga, J. D. & Ratcliffe, E. M. Intestinal microbiota influence the early postnatal development of the enteric nervous system. *Neurogastroenterol Motil* **26**, 98-107, (2014).
49. Aydin, B. *et al.* Gut bacteria-derived succinate induces enteric nervous system regeneration. *bioRxiv*, (2024).
50. Brun, P. *et al.* Toll-like receptor 2 regulates intestinal inflammation by controlling integrity of the enteric nervous system. *Gastroenterology* **145**, 1323-1333, (2013).

51. Yarandi, S. S. *et al.* Intestinal Bacteria Maintain Adult Enteric Nervous System and Nitrergic Neurons via Toll-like Receptor 2-induced Neurogenesis in Mice. *Gastroenterology* **159**, 200-213 e208, (2020).
52. Duncan, M. *et al.* Cannabinoid 1 receptors are critical for the innate immune response to TLR4 stimulation. *Am J Physiol Regul Integr Comp Physiol* **305**, R224-231, (2013).
53. Fitzpatrick, J. M. *et al.* MyD88-dependent and -independent signalling via TLR3 and TLR4 are differentially modulated by Delta(9)-tetrahydrocannabinol and cannabidiol in human macrophages. *J Neuroimmunol* **343**, 577217, (2020).
54. Fitzpatrick, J. K. & Downer, E. J. Toll-like receptor signalling as a cannabinoid target in Multiple Sclerosis. *Neuropharmacology* **113**, 618-626, (2017).
55. Jin, K. *et al.* Defective adult neurogenesis in CB1 cannabinoid receptor knockout mice. *Mol Pharmacol* **66**, 204-208, (2004).
56. Crittenden, J. R., Yoshida, T., Venu, S., Mahar, A. & Graybiel, A. M. Cannabinoid Receptor 1 Is Required for Neurodevelopment of Striosome-Dendron Bouquets. *eNeuro* **9**, (2022).
57. Fitzgerald, M. L., Lupica, C. R. & Pickel, V. M. Decreased parvalbumin immunoreactivity in the cortex and striatum of mice lacking the CB1 receptor. *Synapse* **65**, 827-831, (2011).
58. Rogers, S. A., Kempen, T. A., Pickel, V. M. & Milner, T. A. Enkephalin levels and the number of neuropeptide Y-containing interneurons in the hippocampus are decreased in female cannabinoid-receptor 1 knock-out mice. *Neurosci Lett* **620**, 97-103, (2016).
59. Soriano, D., Vacotto, M., Brusco, A. & Caltana, L. Neuronal and synaptic morphological alterations in the hippocampus of cannabinoid receptor type 1 knockout mice. *J Neurosci Res* **98**, 2245-2262, (2020).
60. Storr, M. A. *et al.* Differential effects of CB(1) neutral antagonists and inverse agonists on gastrointestinal motility in mice. *Neurogastroenterol Motil* **22**, 787-796, e223, (2010).
61. Yuece, B. *et al.* Cannabinoid type 1 receptor modulates intestinal propulsion by an attenuation of intestinal motor responses within the myenteric part of the peristaltic reflex. *Neurogastroenterol Motil* **19**, 744-753, (2007).

62. Sibaev, A. *et al.* Cannabinoid-1 (CB1) receptors regulate colonic propulsion by acting at motor neurons within the ascending motor pathways in mouse colon. *Am J Physiol Gastrointest Liver Physiol* **296**, G119-128, (2009).
63. Lopez-Gomez, L., Szymaszkiewicz, A., Zielinska, M. & Abalo, R. The Enteric Glia and Its Modulation by the Endocannabinoid System, a New Target for Cannabinoid-Based Nutraceuticals? *Molecules* **27**, (2022).
64. Grider, J. R. *et al.* Modulation of motor and sensory pathways of the peristaltic reflex by cannabinoids. *Am J Physiol Gastrointest Liver Physiol* **297**, G539-549, (2009).
65. Barker, H. A. *et al.* Deficiency of cannabinoid receptors enhances host susceptibility to bacterial infection. *mBio* **16**, e0208825, (2025).
66. Cuddihey, H. *et al.* Role of CB(1) receptors in the acute regulation of small intestinal permeability: effects of high-fat diet. *Am J Physiol Gastrointest Liver Physiol* **323**, G219-G238, (2022).
67. Roth, T. D. *et al.* Microbial dysbiosis alters serotonin signaling in a postinflammatory murine model of visceral pain. *Am J Physiol Gastrointest Liver Physiol* **330**, G29-G44, (2026).
68. Arzamendi, M. J. *et al.* Sex-specific post-inflammatory dysbiosis mediates chronic visceral pain in colitis. *Gut Microbes* **16**, 2409207, (2024).
69. Quast, C. *et al.* The SILVA ribosomal RNA gene database project: improved data processing and web-based tools. *Nucleic Acids Res* **41**, D590-596, (2013).